

# A photoplethysmography smartphone-based method for heart rate variability assessment: device model and breathing influences

Federico Guede-Fernández<sup>a,\*</sup>, Víctor Ferrer-Mileo<sup>a</sup>, Marc Mateu-Mateus<sup>a</sup>, Juan Ramos-Castro<sup>a</sup>, Miguel Ángel García-González<sup>a</sup>, Mireya Fernández-Chimeno<sup>a</sup>

<sup>a</sup>*Department of Electronic Engineering, Universitat Politècnica de Catalunya, 08034 Barcelona, Spain*

---

## Abstract

A measurement method of heart rate and heart rate variability (HRV) based on smartphone has been developed and validated. The method is based on photoplethysmography (PPG) acquired with the smartphone camera (SPPG). SPPG was compared with the electrocardiogram (ECG), used as the gold standard, and with an external PPG sensor. Twenty-three healthy subjects were measured using two different smartphone models in three different breathing conditions. The error of the first differentiation between SPPG and ECG series is minimized with the fiducial point at maximum first derivative of the SPPG. The obtained standard deviation of error (SDE) between SPPG and ECG is around 5.4 ms and it is similar to SDE between PPG and ECG. Good agreement between SPPG and ECG for NN, SDNN and RMSSD have been found but it is insufficient agreement for LF/HF. Similar levels of agreement for SPPG-ECG and PPG-ECG have been obtained for the HRV indices. Finally, the differences between smartphone models for HRV indices are slight. Therefore, the smartphone can be used for measuring accurately the following HRV indices: NN, SDNN and RMSSD.

*Keywords:* heart rate variability, mobile application, photoplethysmography, camera

---

## 1. Introduction

The estimated worldwide number of mobile phone lines subscribers were 5.1 billion by the end of 2018, which means two thirds of the world population has access to a smartphone [1]. The widespread use of these devices combined with the improvement of their hardware and software capabilities are enabling a high number of healthcare smartphone applications to reach mass population [2]. The mobile health (mHealth) applications which are focused on fitness and self-monitoring are the most used among people across all ages [3]. As a consequence of mHealth growth, an increasing number of devices for the measurement of vital signs that interface with the smartphone have been presented. An example of those include electrocardiogram (ECG), blood pressure or even photoplethysmography (PPG) [4]. In contrast, there are also mobile applications to measure heart rate (based on PPG) without the need of any external hardware.

PPG is a non-invasive optical measure of the blood volume changes in the microvascular bed of tissues. This method is used to obtain a pulse wave signal which is synchronized with the heartbeat. There are two different types of heart rate (HR) measurements by PPG: contact and non-contact PPG. Contact PPG is based on measuring blood volume changes in the fingertip, while non-contact PPG is based on measuring subtle colour changes on the face of the subject caused by heartbeat [5].

Nowadays, due to the new capabilities of the smartphones, PPG can be acquired using the camera as sensor for monitoring the pulse rate. In this paper, we focus on contact PPG because it has been demonstrated that it has higher feasibility and better accuracy for HR measurement than the non-contact

---

\*Corresponding author

*Email address:* federico.guede@upc.edu (Federico Guede-Fernández)

PPG [6, 7]. There are a high number of mobile phone applications for measuring heart rate from PPG but the accuracy of most of them has not been proven yet. Some of them have been assessed by comparison with ECG, but only the correlation coefficient and standard error of mean HR has been assessed. For this reason, the validity of these measurement systems is limited [8].

Heart rate variability (HRV) is defined as changes in the time interval between consecutive cardiac cycles, which are regulated by the sympathetic and parasympathetic branches of the autonomic nervous system. In addition, there is an increasing research interest on HRV as several relationships between low HRV-associated parameters and some physical and mental health problems have been found. Hypertension, depression and anxiety are some examples [9]. Moreover, HRV can be used to manage physical fatigue and to establish the exercise intensity in athletes [10, 11].

In recent years, there has been an increasing interest in pulse rate variability (PRV) because HRV and PRV indices show high correlation and agreement and no statistically differences, so it can be used as a surrogate of HRV even during non-stationary conditions [12, 13]. In previous research, the Bland-Altman method was used to assess the interchangeability between PRV and HRV indices [14].

Even though there are a number of applications that can perform HRV analysis on the smartphone most of them relay on external sensors. Taking as an example EliteHRV [15], this application acquires the HR intervals from an external HR sensor such as the Polar H7 for HRV analysis instead of using the smartphone camera in order to acquire the HR intervals with the PPG technique.

A review identified eight studies which compared smartphone PPG with ECG or a gold standard PPG using the Bland-Altman method to assess the limits of agreement between them [16]. However, only two of the reviewed studies evaluated the HRV and mean HR: one of them does not show the Bland-Altman (BA) plots and the results, which are only shown in the tables which not seems reliable, because the units of the values of the root mean square of the successive differences (RMSSD) and standard deviation of the NN (R-R) intervals (SDNN) do not agree with normal values [17]. The other study assesses the HRV from an iPhone device, which acquires PPG at a constant frequency [18]. This study only shows the results of correlation and value range of HRV indices and the BA plots of mean HR, SDNN and normalized HF which is not sufficient to validate the method.

Although the aforementioned studies lacked sufficient evidence to validate these methods, there are also a few studies about the accuracy and precision of HRV indices obtained from smartphone based PPG [19, 20, 21, 22] and some preliminary studies to obtain HRV derived from PPG based on other novel methods [23, 24].

This paper presents a study that aimed to evaluate whether the HR derived from PPG acquired with a smartphone allows for reliable estimation of short term HRV indices (5 minutes measurements). Thus, the HRV obtained from smartphone based on contact PPG (SPPG), ECG and PPG acquired with external sensors have been compared. The ECG signal has been considered as the gold standard and the PPG acquired with the external sensor has been considered as a validated PPG method. The error of beat to beat heart period time series obtained with three measurement methods was evaluated. The agreement of HRV indices obtained with the three time series was also assessed. Furthermore, the error with different pulse wave fiducial points has been evaluated and the main possible sources of error have been assessed. In addition, smartphone model and the breathing influences on the measurement have been studied. In order to achieve a proper finger positioning over the lens of camera, a dedicated smartphone case has been designed.

## 2. Materials and methods

### 2.1. Subjects

Twenty-three healthy subjects were recruited for this study among academic staff and university students. The volunteers were healthy, without known cardiac or respiratory diseases and with ages between 22 to 56 years. They were 18 males and 5 females. Their characteristics expressed as (mean  $\pm$  standard deviation) were: weight ( $75.7 \pm 13.9$  kg), height ( $1.74 \pm 0.088$  m) and body mass index ( $24.96 \pm 4.78$  kg/m<sup>2</sup>). All participants gave oral informed consent and this study was performed in accordance with principles of the Declaration of Helsinki [25].

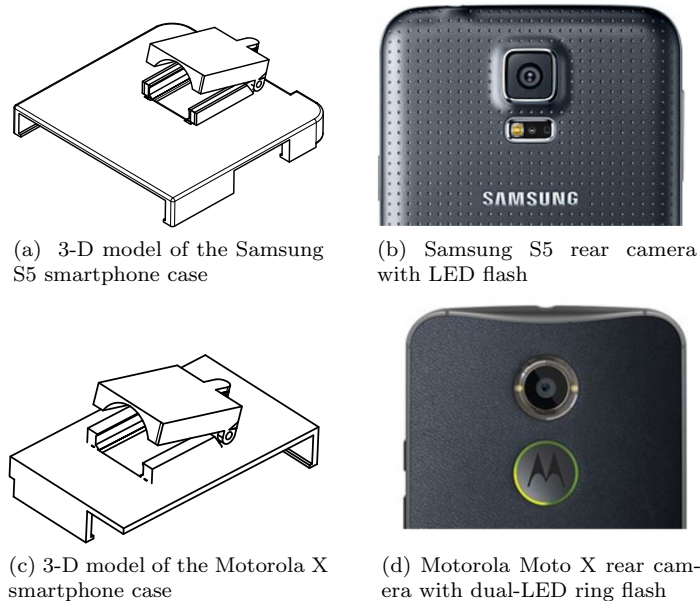


Figure 1: 3-D models of the smartphone cases and the smartphone cameras.

## 2.2. Equipment

### 2.2.1. Smartphone-based photoplethysmography

#### 2.2.1.1. Design of 3-D printed smartphone case for SPPG acquisition application.

For an accurate SPPG signal acquisition and comparison, the finger must be over the flash camera and the camera objective in a proper and reproducible way. In fact, slight finger movements may produce artefacts in the SPPG signal. Hence, a smartphone case has been designed to reduce the signal variability caused by changes in the finger placement. Moreover, it mitigates the ambient light effects over the measurement.

The designed smartphone case has two main components: a rigid case over the smartphone with a hole over the camera sensor and the flash, and a half of thimble that conforms the clamp. The designed smartphone case may aid to obtain more reliable measurements by avoiding unsuitable finger positioning as well as undesirable finger movements. Fig. 1a and Fig. 1c illustrates the 3-D model of the designed smartphone cases for S5 and MX. The rear camera and the LED flash of S5 and MX are shown in Fig. 1b and Fig. 1d respectively.

The smartphone cases have been built using a standard fused deposition modelling (FDM) printer with polylactic acid plastic (PLA) and printed at 100  $\mu\text{m}$  of resolution.

#### 2.2.1.2. Smartphone-based photoplethysmography application.

The SPPG signal has been obtained using a smartphone application developed previously by our research group that is fully described in [26]. Briefly, the smartphone application acquires PPG from the smartphone's built-in rear camera at 30 Hz. The CMOS camera sensor acts as a light detector and the flash as the light source. Changes in the microvascular bed of tissues can be measured by placing the fingertip over the smartphone camera with this non-invasive smartphone-based technique. The SPPG is obtained by processing the green component of each RGB frame [27].

The main blocks of the developed smartphone application are shown in Fig. 2. First, the frame images are acquired in YUV format with NV21 encoding that provide easy and effective compression. Secondly, the Android YUV buffer is converted to RGB pixel array. Thirdly, the green component of the pixel array is averaged to obtain the SPPG waveform. These processing steps have been computed by the smartphone-GPU using Renderscript application programming interface (API). Renderscript API is an Android programming framework that provides a high performance computation because it parallelizes

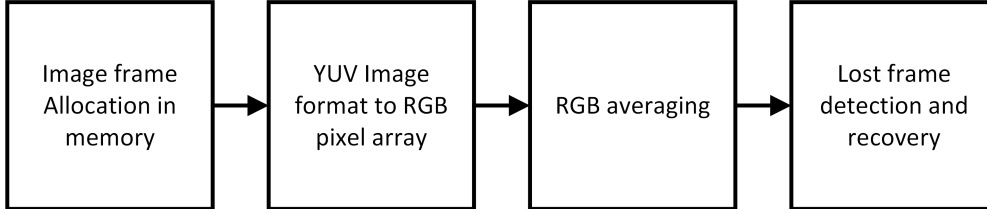


Figure 2: The main processing blocks of the smartphone-based photoplethysmography application

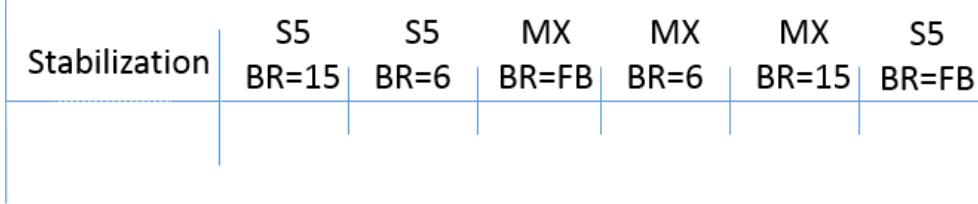


Figure 3: An example of measurement protocol timeline with different smartphone models and breathing rates (BR) for one subject. For each time slot, it is shown the breathing pattern and the smartphone model used.

and schedules work efficiently across available processors of the graphical processing unit (GPU). Thus, the smartphone GPU is used to allocate and process the RGB frames for improving the performance and throughput of acquisition and processing.

### 2.2.2. Physiological data acquisition

The ECG was measured with 3 skin electrodes (3M Red Dot 2560) placed in standard lead I and the pulse signal was measured with a PPG sensor (Biopac SS4LA) placed in the middle finger of the right hand. It is a reflectance type sensor which consists of an infrared emitter and photodiode detector at  $860 \pm 60$  nm wavelengths. The respiratory signal was measured with a respiratory effort transducer (SS5LB). The ECG, PPG and respiratory signal were recorded with a sampling frequency of 5 kHz with a data acquisition device (Biopac MP36E system).

The PPG obtained from the smartphone camera (SPPG) was acquired at 30 Hz on the index finger of the right hand with two different smartphones: Samsung S5 (S5) and Motorola Moto X 2nd generation (MX). The ECG, PPG and SPPG were measured at the same time. MX and S5 present different camera flash LED systems: MX has a dual-LED ring flash and S5 a traditional LED flash. As the position of the LED flash could be a key factor on the acquisition of the SPPG, these two models have been employed to assess the differences related to the choice of the smartphone.

### 2.3. Measurement protocol

A total of 6 measurements were taken for each subject, with three different breathing frequencies for each one of the aforementioned smartphones. The signals were collected at different breathing rates in order to assess the influence of breathing rates in the error of the measurement of the proposed method. It is a well-known fact that respiratory sinus arrhythmia is related to the breathing rate [28]. In this study we wanted to analyze the influence of this arrhythmia in the errors of the HRV derived from the pulse signal. The breathing rates were 6 breaths per minute (bpm), 15 bpm and free breathing. The 6 and 15 bpm breath frequencies were controlled by the means of a visual aid presented to the subject in a smartphone application. Each combination of measurements was randomized and measured for 5 minutes following the recommendation for short-term HRV measurements [29]. The subject was asked to remain seated for the entire experiment because this position is frequently used for this kind of measurements and each subject was asked to perform a 5-minute measurement previous to the actual measurement to stabilize. An example of the timeline of the measurement protocol for one subject is shown in Fig. 3.

Table 1: Cut-off frequencies used in pulse wave algorithm

Fiducial point	High pass frequency (Hz)	Low pass frequency (Hz)
FP 1	0.846	5.303
FP 2	0.107	2.726
FP 3	0.752	3.507

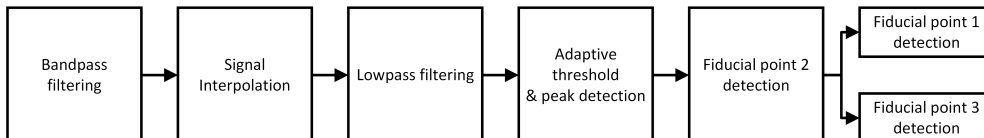


Figure 4: The main processing blocks of the pulse detection algorithm

#### 2.4. ECG, PPG and SPPG Processing: R-to-R and Pulse-to-Pulse time series extraction

The ECG, PPG and SPPG signal were processed offline using MATLAB 2016b in order to obtain the beat-to-beat time series. The Pan-Tompkins QRS complex detector [30] has been used to locate all the R waves (beat to beat) from ECG and then the RR time series have been obtained. After detection, the QRS wave location has been further refined using a template matching correction. A first stage using a coarse detection of the R peak was further refined by maximizing the correlation between the detected peaks and the averaged detected QRS, using 100 ms length templates centered around the coarse fiducial point [31].

The pulse rate from SPPG signal has been detected using three fiducial points. The main blocks of the processing diagram are shown in Fig. 4. Firstly, it has been band-pass filtered using a 4th order bidirectional Butterworth filter to remove the baseline drift and to reduce noise. For each fiducial point, different cut-off frequencies which minimize the standard deviation of the error (SDE) between RR time series extracted from the ECG and PPG found in [32] have been chosen. The values of the cut-off frequencies are shown in Table 1. Secondly, the filtered signal was interpolated from 30 Hz to 5 kHz by a three-point shape-preserving piecewise cubic method in order to achieve the same temporal resolution as PPG and ECG. Thirdly, the interpolated signal is low pass filtered to 10 Hz with a 4th order bidirectional Butterworth filter in order to reduce the noise introduced by the interpolation.

For the detection of the fiducial points an adaptive threshold has been used. The initial value of the threshold is the 50 % of the standard deviation of the first 20 seconds of the first derivative of SPPG. Then, the adaptive threshold is set to 0.4 times the mean of the last three detected SPPG peaks. Additionally, if the detected peak is higher than 1.2 times the average of the last three peaks, the peak value is limited to this value in order to avoid abrupt changes. Finally, the peaks are detected from the maximum value above the threshold of the SPPG first derivative.

The fiducial points, which are shown in Fig. 5, are defined as: minimum of the signal (FP1), maximum of the first derivative (FP2) and maximum of the second derivative (FP3) [33]. Concerning the fiducial point detection, FP2 is the peak detected with the adaptive threshold, regarding the other two fiducial points: the minimum value of the SPPG signal (FP1) or the maximum of the second derivative (FP3) is searched in the 150 ms before the detected peak.

The aforementioned filtering and the mentioned pulse peak detection method have been also used to obtain pulse-to-pulse (PP) time series from the Biopac PPG signal. Fig. 6 shows an example of the acquired signals. The same figure shows the beat-to-beat time intervals which have been obtained for each signal.

#### 2.5. Error Assessment and Statistical Analysis

Since the Biopac system and the smartphone start to measure at different times, prior to error assessment and statistical analysis, the time series RR, PP and SPP should be aligned. Hence, the time series have been

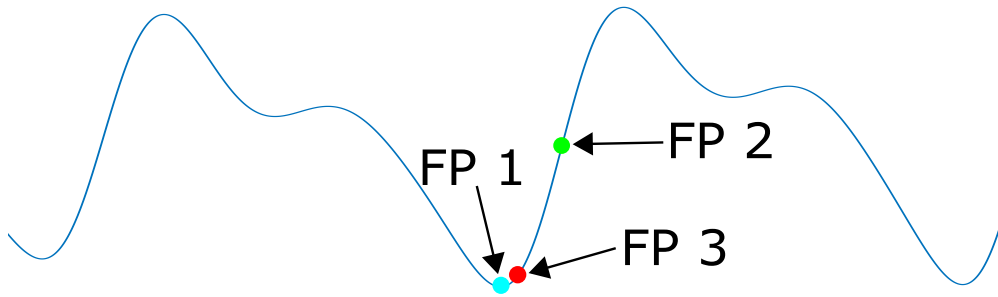


Figure 5: An example of PPG signal with different fiducial points (FP): FP1 is onset of PPG signal, FP2 is the maximum in first derivative of the signal and FP3 is the maximum in second derivative of signal.

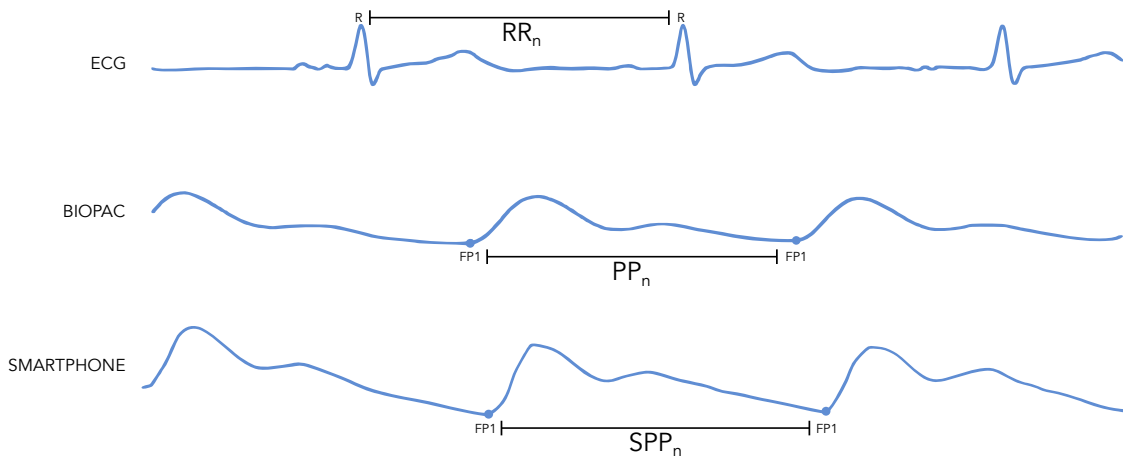


Figure 6: Example of the three measured signals: ECG, PPG and SPPG and the obtained beat-to-beat time interval: RR, PP and SPP.

synchronized and cropped, to align them between each other and to contain the same number of samples. A time series is delayed or advanced respect to the other a finite number of samples until the Fisher intraclass correlation coefficient (ICC) is maximized. Because of the time series are measured simultaneously, we have searched the maximum of ICC by advancing or delaying no more than 10 beats [34].

The artefacts in ECG signal have been visually examined to detect possible outliers in the RR time series. The PP and SPP series have been examined as well by visual inspection. A PP interval is considered as outlier if it differs more than 30 ms from the corresponding RR interval. Finally, the measurements where more than 10% of their PP peaks are outliers or with five consecutive PP outliers have been rejected for analysis. 138 measurements have been recorded (23 subjects x 3 breathing rates x 2 smartphones). 13 measurements from the MX and 1 from the S5 have been discarded due to presence of outliers. Therefore, 124 measurements have been considered in this study.

The standard deviation of error (SDE) has been used to assess the error between the different methods: SPP, PP and RR.

In order to analyse significant differences between pairs of fiducial points, the Mack-Skillings test was computed in every fiducial point-pair [35]. The aforementioned method is an extension of non-parametric two-way Anova Friedman test that is used for unbalanced incomplete block designs, when the number of observations in each treatment/block pair is one or greater, it is an unpaired test. Afterwards, Holm's correction for multiple comparison test has been performed to adjust the p-values [36]. Furthermore, the correlation between different SPP, PP and RR series was assessed with ICC instead of Pearson correlation coefficients, as ICC does not ignore systematic bias.

SDE has also been used to study the influences of smartphone model device and breathing rate. These

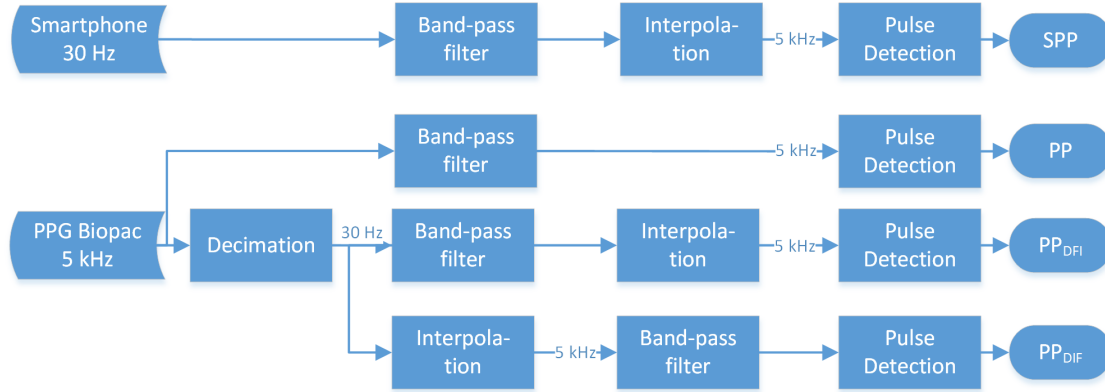


Figure 7: Block diagram of signal conditioning methods before pulse detection. The band-pass filter and interpolation method are the same as detailed in Section 2.4. The decimation technique lowpass filters the input to guard against aliasing and down-samples the result. SPP means smartphone pulse-to-pulse, PP means pulse-to-pulse,  $PP_{DFI}$  means pulse-to-pulse decimated, filtered and interpolated and  $PP_{DIF}$  pulse-to-pulse decimated, interpolated and filtered.

influences were analysed by the means of a non-parametric two-way Anova test (Friedman test). Non-parametric methods were used as the residuals were not normally distributed. For each breath rate, a Friedman test was used to assess smartphone differences. Likewise, for each smartphone, a Friedman test was employed to analyse breath rate differences. Nemeyi post-hoc test has been used to compare breathing rates between each other [37].

Bland-Altman (BA) agreement of HRV indices between these methods has been obtained and the influence of smartphone model has been evaluated. It has been used to assess not only accuracy but also precision of the HRV indices. Mack-Skillings test has also been used to test the differences of HRV indices within smartphone model for all subjects. The mean and standard deviation (SD) of differences and the 95% limits of agreement ( $\pm 1.96$  SD) were calculated. The RR time series has been taken as the gold standard method. The average NN and three short-term HRV indices: SDNN, RMSSD and ratio between power in low frequency and in high frequency (LF/HF) have been computed following the recommendations of Task Force of the European Society of Cardiology [29]. The RR time series was resampled at 4 Hz using cubic spline interpolation and was detrended using a linear polynomial fit. The power spectrum density of HRV was estimated using the Fast Fourier Transform (FFT) and using a Hanning window. The power spectra were computed by calculating the area in two frequency bands: 0.04 to 0.15 Hz for the low frequency (LF) and 0.15 to 0.4 for the high frequency (HF) bands. To quantify the agreement, we have also used the BA ratio which is computed as the half range of limits of agreement divided by the mean of pairwise means of the measurements. Good agreement is defined by a BA ratio  $\leq 10$ , moderate agreement by a BA ratio between 10 and 20, and low agreement by BA  $> 20$  that is insufficient for clinical purposes [38]. The data processing and analysis were performed using R 3.3.1 and MATLAB 2016b.

## 2.6. Assessment of different sources of errors

The deviations of the pulse-to-pulse series obtained with photoplethysmograph and smartphone from the beat-to-beat series derived from ECG can be attributed to a variety of factors such as an unsuitable detection of the pulse period due to system limitations, artefacts, noise or a physiological variability in pulse arrival time (PAT). Fig. 7 shows a block diagram of the processing methods followed to obtain the signals which have been analysed in order to evaluate the sources of error associated to different blocks of the proposed method, the cut-off frequencies of the band-pass filter are the detailed ones in Section 2.4. It must be remarked that the PPG signal obtained from smartphone (SPPG) is sampled at 30 Hz but the ECG and PPG have been acquired at 5 kHz. In order to compare SPPG with the other signals, it has been filtered and interpolated to 5 kHz because decimating the ECG and PPG would result in a loss of relevant information. The different signals obtained were referenced as: SPP, PP,  $PP_{DFI}$  and  $PP_{DIF}$ . The  $PP_{DFI}$  means that the

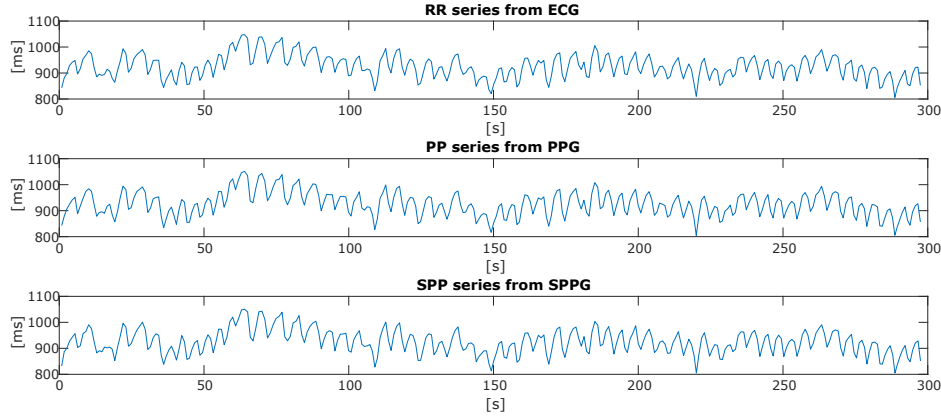


Figure 8: The RR, PP and SPP time series obtained with FP2 of one subject. The SDE between RR and PP is 4.59 ms and between RR and SPP is 4.86 ms

PP series was obtained from PPG that was (in this order) decimated, filtered and interpolated and  $PP_{DIF}$  means that the PP series was (in this order) decimated, interpolated and filtered.

The following sources of error may be distinguished:

1. Errors associated to the signal acquisition method including: hardware (flash light power or location of the camera sensor vs LED) and software (Android OS, designed application ...) limitations of the smartphone, obtained by comparing the SDE of SPP vs  $PP_{DIF}$  as the  $PP_{DIF}$  was obtained from PPG by following the smartphone processing steps.
2. Errors associated to the loss of information of SPP due to a low sampling frequency were obtained by assessing differences of SDE between PP vs  $PP_{DIF}$  as the difference between both series is the processing blocks of the decimation and interpolation.
3. Errors associated to the influence of the sampling frequency in the proposed algorithm were obtained by comparing the differences of the SDE between PP vs  $PP_{DIF}$  as the  $PP_{DIF}$  was first decimated to 30 Hz and then filtered and interpolated to 5 kHz.

### 3. Results

#### 3.1. Comparison of RR and PP series derived from photoplethysmography and smartphone SPP: fiducial point influences

Figure 8 shows an example of one measurement of the RR, PP and SPP time series obtained from ECG, PPG and SPPG respectively and the FP2 was used to obtain PP and SPP time series. Table 2 shows the results of SDE for the RR interval series among ECG, smartphone (SPP) and photoplethysmograph (PP). Using the Mack-Skillings test, statistical significant differences have been found between fiducial points FP2 and FP3 and between FP1 and FP2 for RR-SPP, RR-PP and PP-SPP and between FP1 and FP3 for RR-PP and PP-SPP. The ICC values are similar and close to 1 for all fiducial points. Moreover, the median of SDE with FP2 is lower than FP1 and FP3 in RR-SPP and RR-PP. Therefore, the fiducial point FP2 has been used for the rest of analysis because it shows the lowest error. On the other hand, the median of SDE for RR-PP (4.9 ms) is less than RR-SPP (5.4 ms) but it is greater than PP-SPP (3.95 ms).

#### 3.2. Assessment of different sources of errors

Table 3 shows the results of the standard deviation errors which have been obtained to assess the different sources of errors. These results have been computed with fiducial point 2. The median SDE of  $SPP-PP_{DIF}$  is slightly higher than PP-SPP which was previously shown in Table 2. In addition, the performance of the

Table 2: Standard deviation of error (SDE) and intraclass correlation coefficient (ICC) between RR and SPP, RR and PP and PP and SPP. The pulse has been obtained from different fiducial points (FP)

Fiducial point	RR-SPP	RR-PP	PP-SPP
SDE (ms)			
FP1 (n=124)	6.54 (5–8.48)*	5.42 (4.01–7.99)**, ‡	4.75 (3.93–5.91) ‡‡
FP2 (n=124)	5.4 (4.06–7.35) *, †	4.9 (3.3–6.99) **, †	3.95 (2.98–5.09) ††
FP3 (n=124)	6.2 (4.34–7.89) †	5.24 (3.6–7.86) †, ‡	3.34 (2.59–4.6) ††, ‡‡
ICC			
FP1	0.995 (0.988–0.998)	0.997 (0.993–0.999)	0.998 (0.991–0.999)
FP2	0.997 (0.992–1)	0.998 (0.994–1)	0.999 (0.995–1)
FP3	0.996 (0.99–0.999)	0.997 (0.994–1)	1 (0.997–1)

The data is presented as median IQR (Q25%–Q75%). Holm’s corrected p-values between FP1 and FP2 p<0.05 as “\*” and p<0.001 as “\*\*\*”; between FP2 and FP3 p<0.05 as “†” and p<0.001 as “††”; between FP1 and FP3 p<0.05 as “‡” and p<0.001 as “‡‡”

Table 3: Standard deviation error of SPP and RR by different sources of error for fiducial point 2

Median (Q25%–Q75%) (ms)			
SPP-PP <sub>DFI</sub>	PP- PP <sub>DFI</sub>	PP-PP <sub>DIF</sub>	RR-PP <sub>DFI</sub>
4.01 (3.00–5.01)	0.28 (0.23–0.36)	0 (0–0)*	4.93 (3.31–6.89)

\* Although the median and IQR is 0, the range of error is (0; 0.24)

Table 4: SDE of RR-SPP, RR-PP and PP-SPP by breathing rate and model device

	S5			MX		
	FB (n=22)	BR=6 (n=23)	BR=15 (n=23)	FB (n=18)	BR=6 (n=19)	BR=15 (n=19)
RR-SPP (ms)	5.82 (4.27–7)	5.16 (3.98–6.11)	5.42 (3.87–7.54)	5.26 (3.55–7.84)	5.82 (4.21–7)	6.02 (4.25–8.73)
RR-PP (ms)	4.94 (3.4–6.55)*	5.21 (3.77–6.58)	5.25 (3.74–7.71)*	4.41 (3.18–7.55)	4.73 (2.8–6.84)	4.9 (3.33–7.14)
PP-SPP (ms)	3.15 (2.75–4.62) †	4.17 (3.01–4.88) †	3.35 (2.82–4.35) ‡	3.68 (3.12–4.37)	4.3 (3.55–6.93)	4.72 (3.48–5.74) ‡

BR is breathing rate in breaths per minute and FB means free breathing rate. The results are expressed as median (25%–75% IQR). FB-BR15  $p < 0.05$  as “\*”; FB-BR6  $p < 0.05$  as “†” MX-S5  $p < 0.05$  as “‡”

algorithm for different sampling frequencies (PP-PP<sub>DFI</sub>) is quite similar. Moreover, the error associated to the loss of information due to using a low sampling frequency (PP-PP<sub>DIF</sub>) can be disregarded. The error of RR-PP<sub>DFI</sub> simulates the situation of a validated photoplethysmograph with the same frequency as the smartphone (RR-SPP) and so it isolates the differences associated to both sensors.

### 3.3. Standard deviation of error between RR-SPP, RR-PP and PP-SPP: smartphone and breathing rate influences

Table 4 shows the SDE of time series obtained in different breathing conditions and with both smartphones. Significant statistical differences of the SDE of RR-PP for the smartphone S5 between FB and BR=15 ( $p < 0.05$ ) have been found. Using the Friedman test, it has been found that the differences of SDE SPP-PP are significant for S5 between FB and BR=6 ( $p < 0.05$ ). Concerning the smartphone influences, significant differences have been found on SDE SPP-PP in BR=15 between S5 and MX ( $p < 0.05$ ). Although these differences are significant, they are small, ranging from 0.5 ms to 1 ms approximately. Then, the obtained results are quite similar for both smartphone models in all breathing conditions.

### 3.4. Agreement between SPP-RR, PP-RR and SPP-PP of time and frequency domain HRV indices and smartphone influences

Table 5 shows the results of agreement analysis of HRV indices obtained from SPP, PP and RR. The results have been obtained with the fiducial point 2 which minimizes the SDE between SPP and RR series. To evaluate the smartphone influences on HRV indices, the measurements that are in both smartphones for all combinations of subject and breathing rates have been selected, 14 records were discarded (1 using MX and 13 using S5), remaining 110 measurements. From the Mack-Skillings test, significant differences were found between smartphone models in the NN, SDNN and RMSSD. The 95% confidence of limits of agreement (LA) of NN and SDNN for S5 are lower than for MX but the 95% confidence of LA of RMSSD for S5 is higher than for MX. Moreover, it must be remarked that good agreement has been found for NN, SDNN and RMSSD of SPP-RR but insufficient agreement has been found for LF/HF. Fig. 9 shows the scatter plots of the mean difference and the LA of HRV indices for PP-RR and SPP-RR. This figure shows that data points are scattered uniformly along horizontal axis for NN, SDNN and RMSSD but there is a negative trend of differences, proportional to the magnitude of the measurement in LF/HF for S5 and MX.

## 4. Discussion

The aim of this work was to evaluate whether the HR derived from PPG acquired with a developed smartphone application allows for reliable estimation of HRV indices. The ECG acquired with Biopac has been taken as the reference method. The PPG has been also acquired with the Biopac system in order to

Table 5: Bland-Altman agreement analysis between SPP, RR and PP of HRV indices for each smartphone model

	SPP-RR		PP-RR		SPP-PP	
	S5	MX	S5	MX	S5	MX
NN (ms)	0.06 ± 1.64	0.3 ± 2.72‡	-0.37 ± 1.83	0.07 ± 3.11	0.43 ± 1.88	0.23 ± 3.44
SDNN (ms)	1.19 ± 2.75	1.68 ± 2.79‡	0.97 ± 3.07	0.74 ± 4.42	0.22 ± 1.79	0.93 ± 4.11‡
RMSSD (ms)	1.43 ± 4.07	2.91 ± 3.56‡‡	0.81 ± 5.87	1.2 ± 5.01	0.62 ± 4.37	1.7 ± 4.33‡‡
LF/HF (n.u)	-0.7 ± 4.1	-1.3 ± 5.62	-0.49 ± 4.53	-0.45 ± 3.21	-0.2 ± 2.14	-0.85 ± 4.29
BA ratio						
NN (%)	0.18	0.29	0.2	0.34	0.2	0.37
SDNN (%)	3.87	3.86	4.33	6.16	2.5	5.66
RMSSD (%)	7.15	6.15	10.36	8.79	7.62	7.42
LF/HF (%)	52.35	66.43	57.16	36.07	28.25	52

Bias ± 95% confidence of limits of agreement. Means difference statistical p-value: p<0.05 as “‡” and p<0.001 as “‡‡”

obtain the agreement with ECG. Then, we have compared the agreement of the PPG obtained with the developed application and the PPG and ECG from the reference.

The standard deviation of error of SPP and PP series has been obtained for each fiducial point. The lowest SDE has been obtained with FP2 but the differences are small (around 1 ms). For this fiducial point, the error made in the estimation of the RR time series using the smartphone (RR-SPP=5.4 ms) is only a 10% bigger than using a photoplethysmograph (RR-PP=4.9 ms). As it was expected, because of PP and SPP are derived from pulse wave signals, the median of SDE PP-SPP (3.95 ms) is lower than RR-PP which is lower than SPP-RR.

The possible sources of error between the smartphone and the photoplethysmograph are the different sampling frequency and the employed device. Regarding the first, the results obtained when the pulse signal (PPG) is subsampled to 30 Hz, have shown that if a spline interpolation procedure is applied the information loss due to this frequency is negligible. Therefore, the SPPG signal (30 Hz) must be filtered to reduce the noise before being interpolated to 5 kHz. In addition, it has been assessed that the error produced when the pulse detection algorithm is employed with a low sample frequency (30 Hz and free of noise) the error is low (0.28 ms).

Concerning the device employed, the SDE between them (SPP-PP) is around 4 ms. This SDE is not only associated with the smartphone, otherwise the SDE between RR-SPP and RR-PP would be greater. Some of this error may be related to how the measurement is performed, or even due to the variability in the pulse arrival time (PAT). Hence, the error in the smartphone (RR-SPP) is not only associated with the device but it is also related with PAT and how the measurement was performed.

The SDE for different smartphone models and breathing rates has been assessed in order to study their influence on SPPG and PPG measurements. Although some SDE differences between breathing rates has been found significant, they are small as they range from 0.5 to 1 ms. The SDE of both smartphone models are similar.

The HRV indices obtained from SPP, PP and RR series have been compared. The Bland-Altman analysis performed shows not only the accuracy but also the precision. The agreement of HRV indices when comparing SPP-RR are slightly less accurate but more precise than PP-RR. It can be caused by the difference in the measured finger, as the PP is measured on the middle finger but SPP is measured on the index finger. The BA ratio has shown good agreement for NN, SDNN and RMSSD but insufficient agreement for LF/HF in all comparisons. The LF/HF ratio from PP and SPP decreased in comparison with the LF/HF obtained from RR. This decrease could be associated to the respiratory sinus arrhythmia components. These

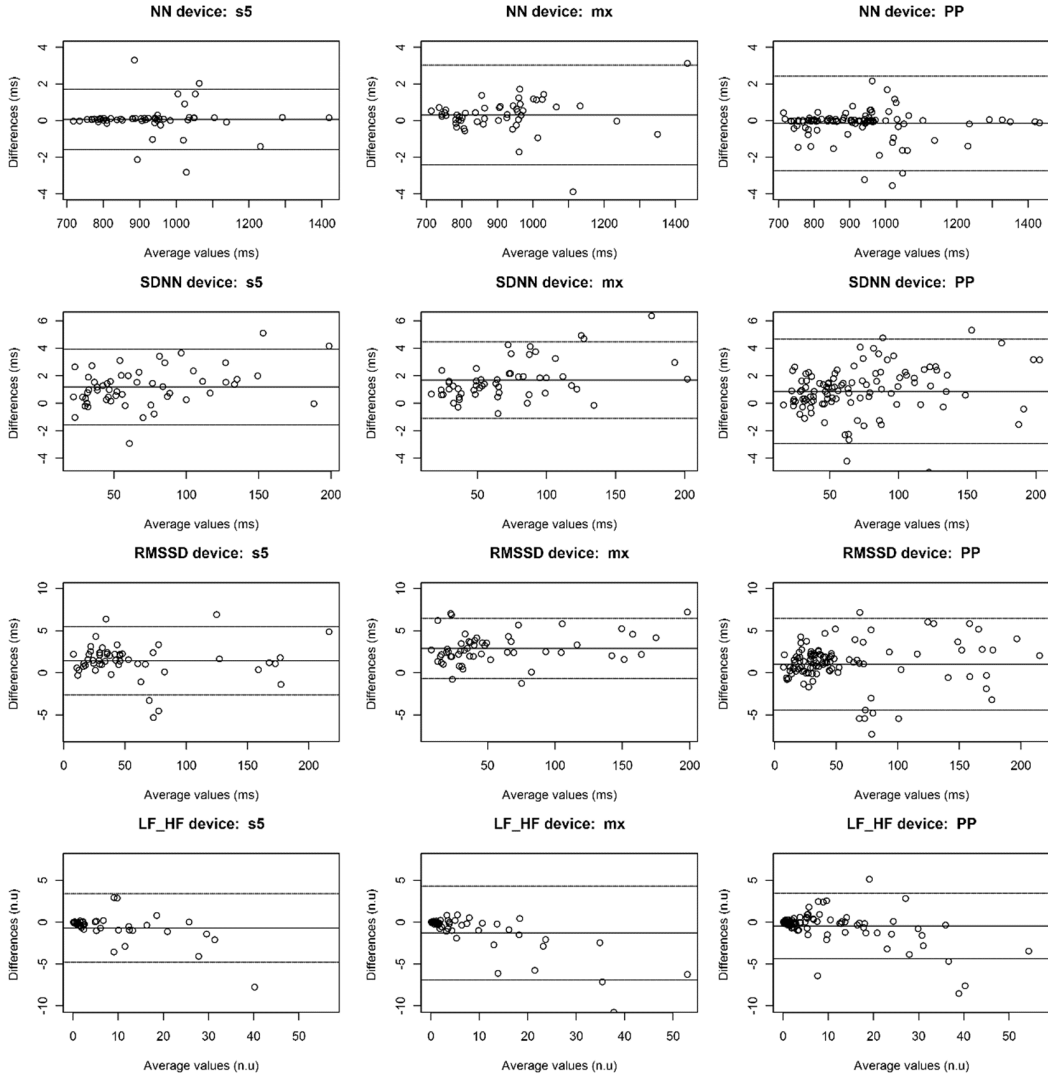


Figure 9: Bland-Altman bias and limits of agreement of HRV indices. The first column shows the agreement between  $SPP_{S5}$  and RR, the second column  $SPP_{MX}$ -RR and third column PP-RR.

components (high frequency activity) may be more pronounced in the PPG and smartphone signal and so, the LF/HF of PP and SPP may decrease [39].

The BA shows that for SPP-RR the bias and precision of NN, SDNN, RMSSD and LF/HF are quite similar for S5 and MX. The obtained LA and BA ratio of SPP-RR HRV indices are better than the previously reported in a similar study [19]. A possible explanation for these differences might be that the instantaneous frame rate of the mentioned study oscillated between 20 and 30 Hz and in our smartphone camera algorithm it was around 30 Hz.

An iPhone smartphone application for HRV analysis based on camera PPG was shown in [21]. In the aforementioned study, the relationship between HR, HRV and self-reported training was evaluated but the assessment of accuracy of this method was not studied. This smartphone application was assessed by

comparison with ECG [22]. However, only the result of RMSSD index was assessed, it shows the standardized difference has also been computed 0.06 (0.05; 0.08), in contrast the standardized mean difference which was obtained with our method was 0.044 (-0.179; 0.268). Their measurements have a duration of 1 minute whereas our measurements have a duration of 5 minutes, which is the duration established by the norm for short term HRV assessment.

A review of heart rate measurement methods based on smartphone which was previously published [16], shows the results of the mean difference, the Pearson correlation and the level of agreement between heart rate measured by a smartphone and a validated method of the reviewed studies. A total number of 14 publications were included in this review.

The mean difference of the heart rate obtained with our method was 0.011 beats per minute and 99% CI (-0.1500; 0.1734). In addition, the Pearson correlation obtained with our method was  $>0.99$  an  $p\text{-value} < 0.001$ . The obtained 95% levels of agreement in beats per minute were (-0.1114; 0.1347) which are lower than the studies reviewed in [16]. Therefore, the results which have been obtained with our method are better than the reviewed studies. These obtained results may be better than the reviewed studies because the cut-off frequencies, which were used for the band pass filter of the proposed method, were optimized in order to minimize the error.

A limitation of this study was that the participants were guided to follow the different breathing rates (6 bpm and 15 bpm) with graphical animations in the smartphone application, this guidance indicated the time to inhale and exhale in accordance with the fixed breathing rate. The experiment supervisor checked that the participants followed the graphical indications and the respiratory signal was acquired and analysed to corroborate the different breathing conditions. Guided breathing rates are a limitation because the subject must to concentrate to synchronize his/her breathing with an external signal. Such an effort can modify the dynamics of the analyzed time series as suggested in [40].

## 5. Conclusion

The differences among smartphone-based PPG, ECG and reference PPG have been assessed. The error between SPP and RR series is minimized with fiducial point at maximum of first derivate (FP2). The error caused by the sampling rate of smartphone camera (30 Hz) is compensated with the interpolation method. The obtained SDE between SPP and RR is around 5.4 ms, it is similar to SDE between PP and RR. In addition, similar SDE has been obtained for both smartphone models in the three breathing rates. On the other hand, the levels of agreement between the methods: smartphone, ECG and PPG have been obtained. Similar levels of agreement for SPP-RR and PP-RR have been obtained for NN, SDNN, RMSSD and LF/HF. Good agreement of SPP-RR for NN, SDNN and RMSSD have been found but insufficient agreement of LF/HF. Finally, the SPP-RR differences between smartphone models of 95% limits of agreement for SDNN, RMSSD and LF/HF are slight. Therefore, the smartphone can be used for measuring NN, SDNN and RMSSD accurately and differences between smartphone models are small.

## Acknowledgements

This work has been partially financed by the Spanish Ministry of Economy, Industry and Competitiveness, DEP2015-68538-C2-2-R.

## References

- [1] GSMA Intelligence, The Mobile Economy 2019, Tech. rep. (2019).  
URL <https://www.gsma.com/r/mobileeconomy/>
- [2] S. P. Bhavnani, J. Narula, P. P. Sengupta, Mobile technology and the digitization of healthcare, *European Heart Journal* 37 (18) (2016) 1428–1438.  
URL <http://dx.doi.org/10.1093/eurheartj/ehv770>
- [3] P. R. Sama, Z. J. Eapen, K. P. Weinfurt, B. R. Shah, K. A. Schulman, An evaluation of mobile health application tools., *JMIR mHealth and uHealth* 2 (2) (2014) e19. doi:10.2196/mhealth.3088.

- [4] J. A. J. Heathers, Smartphone-enabled pulse rate variability: An alternative methodology for the collection of heart rate variability in psychophysiological research, *International Journal of Psychophysiology* 89 (3) (2013) 297–304. doi:<http://dx.doi.org/10.1016/j.ijpsycho.2013.05.017>. URL <http://www.sciencedirect.com/science/article/pii/S0167876013001694>
- [5] Y. Sun, N. Thakor, Photoplethysmography Revisited: From Contact to Noncontact, From Point to Imaging, *IEEE Transactions on Biomedical Engineering* 63 (3) (2016) 463–477. doi:10.1109/TBME.2015.2476337.
- [6] M. T. I. Papon, I. Ahmad, N. Saquib, A. Rahman, Non-invasive heart rate measuring smartphone applications using on-board cameras: A short survey, in: 2015 International Conference on Networking Systems and Security (NSysS), 2015, pp. 1–6. doi:10.1109/NSysS.2015.7043533.
- [7] T. Coppetti, A. Brauchlin, S. Muggler, A. Attinger-Toller, C. Templin, F. Schonrath, J. Hellermann, T. F. Luscher, P. Biaggi, C. A. Wyss, Accuracy of smartphone apps for heart rate measurement., *European journal of preventive cardiology* 24 (12) (2017) 1287–1293. doi:10.1177/2047487317702044.
- [8] R. W. Treskes, E. T. van der Velde, R. Barendse, N. Bruining, Mobile health in cardiology: a review of currently available medical apps and equipment for remote monitoring., *Expert review of medical devices* 13 (9) (2016) 823–830. doi:10.1080/17434440.2016.1218277.
- [9] A. L. Wheat, K. T. Larkin, Biofeedback of heart rate variability and related physiology: a critical review., *Applied psychophysiology and biofeedback* 35 (3) (2010) 229–242. doi:10.1007/s10484-010-9133-y.
- [10] J.-G. DONG, The role of heart rate variability in sports physiology, *Experimental and Therapeutic Medicine* 11 (5) (2016) 1531–1536. doi:10.3892/etm.2016.3104. URL <http://www.ncbi.nlm.nih.gov/pmc/articles/PMC4840584/>
- [11] S. Evans, L. C. Seidman, J. C. Tsao, K. C. Lung, L. K. Zeltzer, B. D. Naliboff, Heart rate variability as a biomarker for autonomic nervous system response differences between children with chronic pain and healthy control children., *Journal of pain research* 6 (2013) 449–457. doi:10.2147/JPR.S43849.
- [12] E. Gil, M. Orini, R. Bailon, J. M. Vergara, L. Mainardi, P. Laguna, Photoplethysmography pulse rate variability as a surrogate measurement of heart rate variability during non-stationary conditions., *Physiological measurement* 31 (9) (2010) 1271–1290. doi:10.1088/0967-3334/31/9/015.
- [13] C.-C. Chuang, J.-J. Ye, W.-C. Lin, K.-T. Lee, Y.-T. Tai, Photoplethysmography variability as an alternative approach to obtain heart rate variability information in chronic pain patient., *Journal of clinical monitoring and computing* 29 (6) (2015) 801–806. doi:10.1007/s10877-015-9669-8.
- [14] H. F. Posada-Quintero, D. Delisle-Rodriguez, M. B. Cuadra-Sanz, R. R. Fernandez de la Vara-Prieto, Evaluation of pulse rate variability obtained by the pulse onsets of the photoplethysmographic signal., *Physiological measurement* 34 (2) (2013) 179–187. doi:10.1088/0967-3334/34/2/179.
- [15] A. S. Perrotta, A. T. Jeklin, B. A. Hives, L. E. Meanwell, D. E. R. Warburton, Validity of the Elite HRV Smartphone Application for Examining Heart Rate Variability in a Field-Based Setting., *Journal of strength and conditioning research* 31 (8) (2017) 2296–2302. doi:10.1519/JSC.0000000000001841.
- [16] B. De Ridder, B. Van Rompaey, K. J. Kampen, S. Haïne, T. Dilles, Smartphone Apps Using Photoplethysmography for Heart Rate Monitoring: Meta-Analysis, *JMIR Cardio* 2 (1) (2018) e4. doi:10.2196/cardio.8802. URL <http://cardio.jmir.org/2018/1/e4/> <http://www.ncbi.nlm.nih.gov/pubmed/>
- [17] J. B. Bolkhovsky, C. G. Scully, K. H. Chon, Statistical analysis of heart rate and heart rate variability monitoring through the use of smart phone cameras., *Conference proceedings : ... Annual International Conference of the IEEE Engineering in Medicine and Biology Society. IEEE Engineering in Medicine and Biology Society. Annual Conference 2012* (2012) 1610–1613. doi:10.1109/EMBC.2012.6346253.
- [18] N. Koenig, A. Seeck, J. Eckstein, A. Mainka, T. Huebner, A. Voss, S. Weber, Validation of a new heart rate measurement algorithm for fingertip recording of video signals with smartphones, *Telemedicine and e-Health* 22 (8) (2016) 631–636.
- [19] R.-C. Peng, X.-L. Zhou, W.-H. Lin, Y.-T. Zhang, Extraction of Heart Rate Variability from Smartphone Photoplethysmograms, *Computational and Mathematical Methods in Medicine* 2015 (2015) 1–11. doi:10.1155/2015/516826. URL <http://www.hindawi.com/journals/cmmm/2015/516826/>
- [20] A. Bánhalmi, J. Borbás, M. Fidirich, V. Bilicki, Z. Gingl, L. Rudas, Analysis of a Pulse Rate Variability Measurement Using a Smartphone Camera, *Journal of Healthcare Engineering* 2018.
- [21] M. Altini, O. Amft, HRV4Training: Large-scale longitudinal training load analysis in unconstrained free-living settings using a smartphone application., *Conference proceedings : ... Annual International Conference of the IEEE Engineering in Medicine and Biology Society. IEEE Engineering in Medicine and Biology Society. Annual Conference 2016* (2016) 2610–2613. doi:10.1109/EMBC.2016.7591265.
- [22] D. J. Plews, B. Scott, M. Altini, M. Wood, A. E. Kilding, P. B. Laursen, Comparison of heart-rate-variability recording with smartphone photoplethysmography, polar H7 chest strap, and electrocardiography, *International Journal of Sports Physiology and Performance* 12 (10) (2017) 1324–1328. doi:10.1123/ijsp.2016-0668. URL <http://journals.humankinetics.com/doi/10.1123/ijsp.2016-0668>
- [23] V. R. Pamula, M. Verhelst, C. V. Hoof, R. F. Yazicioglu, A novel feature extraction algorithm for on the sensor node processing of compressive sampled photoplethysmography signals, in: 2015 IEEE SENSORS, 2015, pp. 1–4. doi:10.1109/ICSENS.2015.7370396.
- [24] S. M. A. Salehizadeh, D. Dao, J. Bolkhovsky, C. Cho, Y. Mendelson, K. H. Chon, A Novel Time-Varying Spectral Filtering Algorithm for Reconstruction of Motion Artifact Corrupted Heart Rate Signals During Intense Physical Activities Using a Wearable Photoplethysmogram Sensor, *Sensors (Basel, Switzerland)* 16 (1) (2015) 10. doi:10.3390/s16010010. URL <https://www.ncbi.nlm.nih.gov/pubmed/26703618> <https://www.ncbi.nlm.nih.gov/pmc/articles/PMC4732043/>
- [25] World Medical Association, World Medical Association Declaration of Helsinki. Ethical principles for medical research

- involving human subjects., *Bulletin of the World Health Organization* 79 (4) (2001) 373–374.  
 URL <http://www.ncbi.nlm.nih.gov/pmc/articles/PMC2566407/>
- [26] F. Guede-Fernandez, V. Ferrer-Mileo, J. Ramos-Castro, M. Fernandez-Chimeno, M. Garcia-Gonzalez, Real time heart rate variability assessment from Android smartphone camera photoplethysmography: Postural and device influences, in: *Proceedings of the Annual International Conference of the IEEE Engineering in Medicine and Biology Society, EMBS*, Vol. 2015-Novem, Milan, 2015, pp. 7332–7335. doi:10.1109/EMBC.2015.7320085.
- [27] K. Matsumura, P. Rolfe, J. Lee, T. Yamakoshi, iPhone 4s photoplethysmography: which light color yields the most accurate heart rate and normalized pulse volume using the iPhysioMeter Application in the presence of motion artifact?, *PloS one* 9 (3) (2014) e91205. doi:10.1371/journal.pone.0091205.
- [28] A. Beda, D. M. Simpson, N. C. Carvalho, A. R. S. Carvalho, Low-frequency heart rate variability is related to the breath-to-breath variability in the respiratory pattern., *Psychophysiology* 51 (2) (2014) 197–205. doi:10.1111/psyp.12163.
- [29] Task Force of the European Society of Cardiology and the North American Society of Pacing and Electrophysiology, *Heart Rate Variability : Standards of Measurement, Physiological Interpretation, and Clinical Use* (1996). arXiv:WOS:A1996UF54400011, doi:10.1161/01.CIR.93.5.1043.
- [30] J. Pan, W. J. Tompkins, A real-time QRS detection algorithm., *IEEE transactions on bio-medical engineering* 32 (3) (1985) 230–236. doi:10.1109/TBME.1985.325532.
- [31] B. . Kohler, C. Hennig, R. Orglmeister, The principles of software QRS detection, *IEEE Engineering in Medicine and Biology Magazine* 21 (1) (2002) 42–57. doi:10.1109/51.993193.
- [32] V. Ferrer-Mileo, F. Guede-Fernandez, M. Fernandez-Chimeno, J. Ramos-Castro, M. A. Garcia-Gonzalez, Accuracy of heart rate variability estimation by photoplethysmography using an smartphone: Processing optimization and fiducial point selection, in: *2015 37th Annual International Conference of the IEEE Engineering in Medicine and Biology Society (EMBC)*, Vol. 2015-Novem, IEEE, 2015, pp. 5700–5703. doi:10.1109/EMBC.2015.7319686.  
 URL <https://ieeexplore.ieee.org/document/7319686/>
- [33] Y. C. Chiu, P. W. Arand, S. G. Shroff, T. Feldman, J. D. Carroll, Determination of pulse wave velocities with computerized algorithms, *American heart journal* 121 (5) (1991) 1460–1470.
- [34] M. García-González, M. Fernández-Chimeno, F. Guede-Fernández, V. Ferrer-Mileo, A. Argelagós-Palau, L. Álvarez-Gómez, E. Parrado, J. Moreno, L. Capdevila, J. Ramos-Castro, A methodology to quantify the differences between alternative methods of heart rate variability measurement, *Physiological Measurement* 37 (1). doi:10.1088/0967-3334/37/1/128.
- [35] G. A. Mack, J. H. Skillings, A Friedman-Type Rank Test for Main Effects in a Two-Factor ANOVA, *Journal of the American Statistical Association* 75 (372) (1980) 947–951. doi:10.1080/01621459.1980.10477577.  
 URL <http://www.tandfonline.com/doi/abs/10.1080/01621459.1980.10477577>
- [36] S. Holm, A Simple Sequentially Rejective Multiple Test Procedure, *Scandinavian Journal of Statistics* 6 (2) (1979) 65–70.  
 URL <http://www.jstor.org/stable/4615733>
- [37] P. Nemenyi, Distribution-free multiple comparisons, in: *Biometrics*, Vol. 18, INTERNATIONAL BIOMETRIC SOC 1441 I ST, NW, SUITE 700, WASHINGTON, DC 20005-2210, 1962, p. 263.
- [38] S. W. Weinschenk, R. D. Beise, J. Lorenz, Heart rate variability (HRV) in deep breathing tests and 5-min short-term recordings: agreement of ear photoplethysmography with ECG measurements, in 343 subjects, *European Journal of Applied Physiology* 116 (8) (2016) 1527–1535. doi:10.1007/s00421-016-3401-3.  
 URL <http://link.springer.com/10.1007/s00421-016-3401-3>
- [39] W. Karlen, C. J. Brouse, E. Cooke, J. M. Ansermino, G. A. Dumont, Respiratory rate estimation using respiratory sinus arrhythmia from photoplethysmography, in: *2011 Annual International Conference of the IEEE Engineering in Medicine and Biology Society, IEEE*, 2011, pp. 1201–1204. doi:10.1109/IEMBS.2011.6090282.  
 URL <http://ieeexplore.ieee.org/document/6090282/>
- [40] Y.-J. Park, Y.-B. Park, Clinical utility of paced breathing as a concentration meditation practice, *Complementary Therapies in Medicine* 20 (6) (2012) 393–399. doi:https://doi.org/10.1016/j.ctim.2012.07.008.  
 URL <http://www.sciencedirect.com/science/article/pii/S0965229912001148>